A Novel Crossed Traveling Wave Induction Heating System and Finite Element Analysis of Eddy Current and Temperature Distributions

S. L. Ho[1], Junhua Wang[1], W. N. Fu[1], and Y. H. Wang[2]

[1]Department of Electrical and Engineering, The Hong Kong Polytechnic University, Hunghom, Kowloon, Hong Kong
[2]Joint Key Lab. of Electromagnetic Field and Electrical Apparatus Reliability, Hebei Univ. of Technology, Tianjin, 300130, China

A novel crossed traveling wave induction heating (C-TWIH) system for heating thin industrial strips is proposed and its finite element method (FEM) simulations are reported. Compared with a typical traveling wave induction heating (TWIH) device, C-TWIH has more uniform and concentrated eddy current density distributions. This is because the C-TWIH system exploits a three-phase induction heater with crossed yoke arrangement, and the magnetic fluxes generated by each phase are interacting and complementing each other to compensate for the weak magnetic areas of each phase. Temperature distribution and variation of the C-TWIH system is also characterized. The fabricated novel model has a temperature range from 251°C to 270°C and its undesired temperature non-uniformity is reduced by 43% compared with those in typical TWIH devices.

Index Terms—**Eddy current, finite element method, temperature distribution, transverse flux, traveling wave.**

I. Introduction

THE INCREASING demand for industrial furnace heaters has attracted a lot of attentions from researchers and practitioners. Traditional longitudinal method and single- phase transverse flux technology are inadequate to meet the ever increasing demand on quality performance in regard to temperature uniformity on the work strips, especially on thin and long strips. Among the multiphase systems being developed recently, the traveling wave induction heating (TWIH) process is potentially very promising and attractive.

Unlike the longitudinal or the single-phase transverse flux heaters, TWIH is energized with three-phase windings. Parametric analysis is used to assess the key parameters (transmission efficiency of electricity to the work-piece, power factor, etc.). TWIH is intrinsically more suitable than its single phase counterpart in the provision of uniform thermal density on the work strips [1]. Indeed, three-phase induction heaters not only have the same advantages as their single-phase counterparts, they can produce more uniform temperature distributions and operate with less industrial noise and vibration. For operations in which the electromagnetic force may increase significantly and the heating parameters could change as the temperature rises, the advantage of TWIH is even more significant.

Despite of the wealth of industrial potential applications of TWIH, there are few reports in the literatures on this important technology when compared to those on longitudinal induction heating and transverse flux induction heating (TFIH) systems, even though there are some dedicated analytical studies and numerical methods on TWIH systems [2]–[5]. In fact, prior studies only introduce some unrealistically over-simplified and impractical assumptions using, for example, a current sheet on the yoke without slots as the model.

A novel design for a crossed traveling wave induction heating (C-TWIH) system is proposed to address the inhomogeneous eddy current density which dominates the temperature distribution on the surface of work strips. Finite element method (FEM) is used to calculate the eddy current and temperature distributions. Simulation results of the novel C-TWIH system are presented and compared with those of typical TWIH and TFIH systems to showcase its better performance.

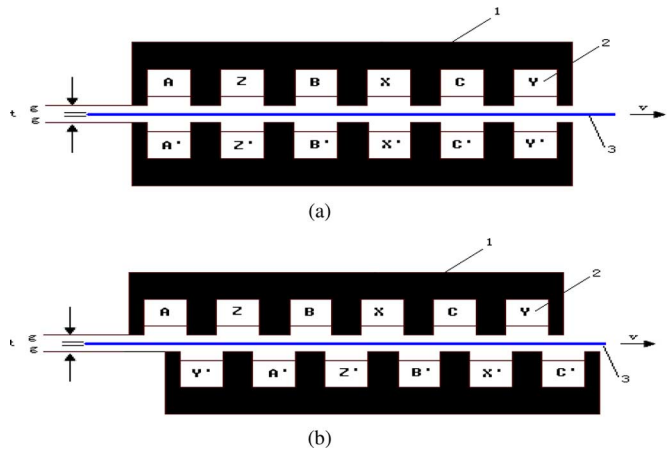

Fig. 1. (a) Schematic of a typical double-sided TWIH system; (b) Schematic of the double-sided C-TWIH system (1-magnetic yoke; 2-exciting windings; 3-load metal sheet; t-strip thickness; g-airgap between inductor and load; v-strip movement velocity. Phase degree: $A - X$ and $A' - X' = 0°$, $B - Y$ and $B' - Y' = -120°$, $C - Z$ and $C' - Z' = -240°$).

II. Proposed Structure of C-TWIH

The schematic of a typical heater configuration is shown in Fig. 1(a). There are two linear inductors on the opposite sides of the strip and twelve slots along the direction of the movement. There is a relatively large airgap between the inductor and the strip due to the thickness of the interposing refractory materials.

The proposed C-TWIH system is shown in Fig. 1(b). With this structure the lower inductor is shifted 60 degrees along the movement direction of the strip and the winding starts from phase Y'. On each inductor there are three phases and six windings. Alternating current through every two in-phase sets of windings sets up the magnetic field, which is perpendicular to

Manuscript received March 06, 2009. Current version published September 18, 2009. Corresponding author: J. Wang (e-mail: junhua.wong@polyu.edu.hk, 08900600r@polyu.edu.hk).

Color versions of one or more of the figures in this paper are available online at http://ieeexplore.ieee.org.

Digital Object Identifier 10.1109/TMAG.2009.2021667

TABLE I
DESIGN DATA OF TYPICAL TWIH AND C-TWIH HEATERS OF FIG. 1

Number of phases	3
Number of windings	6
Number of slots	12
Airgap distance *(g)*	1.0 mm
Magnetic yoke length	1300mm
Magnetic yoke height	200mm
Aluminum strip width	130 mm
Aluminum strip thickness *(t)*	2.0 mm
Strip movement velocity *(v)*	1.0 m/min

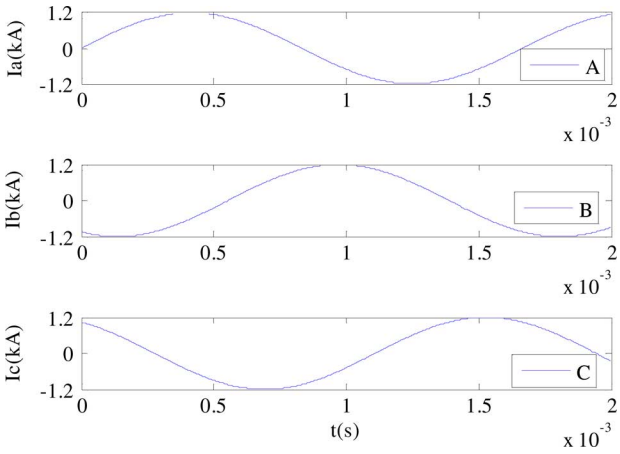

Fig. 2. Three-phase exciting current waveforms for typical TWIH and C-TWIH systems.

the surface of the sheet, and eddy currents are induced by the alternating magnetic flux on the work strip.

In the following FEM simulation, the amplitude of the exciting current is 1200 A at 600 Hz. The phase current waveforms are as shown in Fig. 2.

It can be seen from Figs. 1 and 2 that at any instant, there are always four inductor phase windings acting as the field windings to generate the flux in the C-TWIH device; while in typical TWIH device, there are two phase windings only.

III. SIMULATION OF SYSTEM PERFORMANCE

In this section, the operation of the two three-phase induction heating devices, namely the typical TWIH and C-TWIH, with the phase currents of Fig. 2 are investigated using FEM analysis. Particular attention is paid to the analysis of the magnetic flux density, eddy current distribution, power density and the temperature field.

A. Magnetic Flux Density Analysis

Because AC current through every winding generates a magnetic field, which induces eddy currents to produce the thermal field, the total magnetic field is the additive contribution of six upper-and-lower windings.

$$\oint Hdl = \sum i = N_c i \tag{1}$$

where N_c is the number of turns per phase per winding, and

$$i = \sqrt{2} I \sin(\omega t + \theta) \tag{2}$$

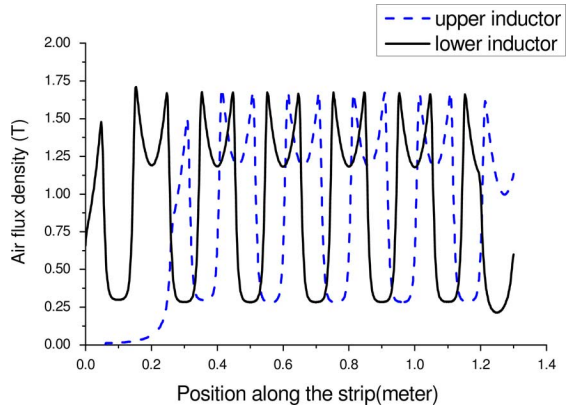

Fig. 3. Airgap flux density distribution in the work strip from the upper and lower inductors.

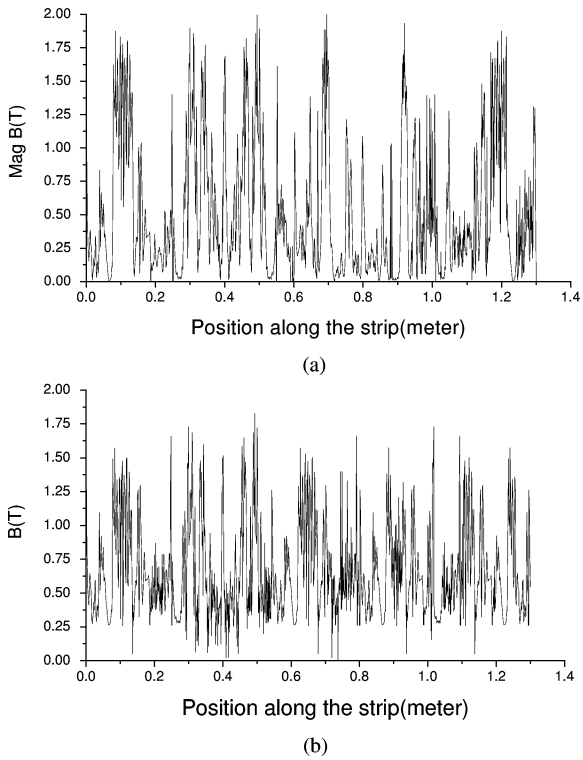

Fig. 4. Magnetic flux density distribution in the work strip. (a) In typical TWIH system, (b) In C-TWIH system.

where I is the r.m.s. current and θ is the phase angle.

The result of the airgap flux density calculation of the C-TWIH system is shown at different positions in Fig. 3. The average trend of the airgap flux density B has a symmetrical waveform having similarly triangle-topped amplitude. Flux densities in the upper and lower inductors make up for the weak areas of each other. This leads to a more uniform eddy current density in the work strips, as discussed in Part B.

The magnetic flux densities in the work strip of the C-TWIH system are depicted in Fig. 4(b). In order to study the efficiency of the C-TWIH system, the flux density distribution along the work strips of a typical TWIH system is also calculated, which is shown in Fig. 4(a).

It can be seen that typical TWIH system's magnetic flux is distributed symmetrically along both sides of the axis and

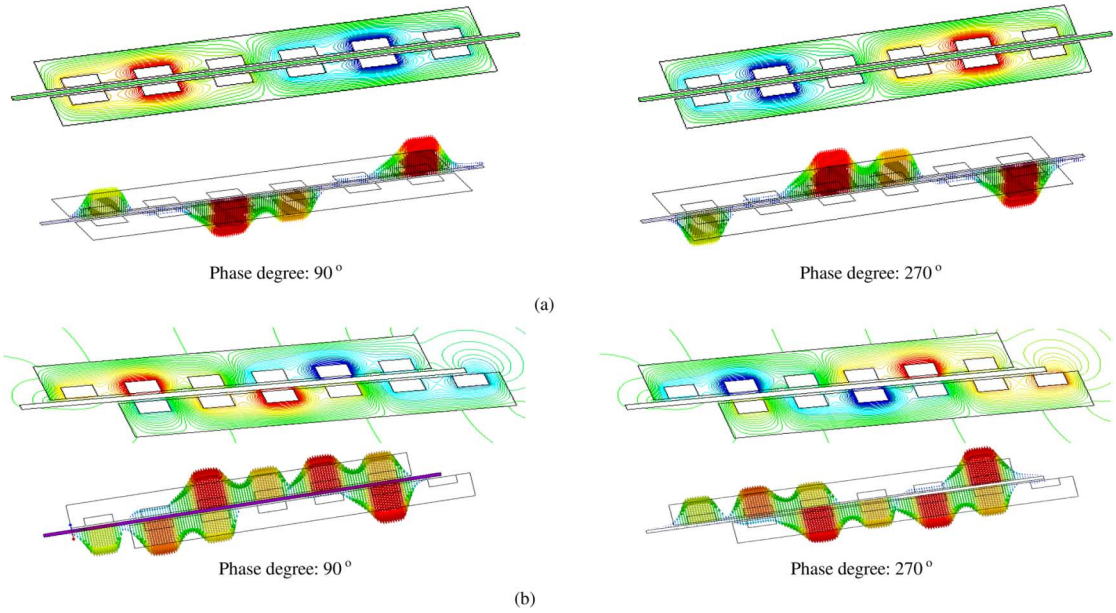

Fig. 5. Magnetic flux distributions in the strip and induced power density distributions along the direction of the strip movement (yoke size—1300 × 30 mm; slot size—150 × 50 mm; airgap—1 mm; strip thickness-2 mm; currents supply $I - l200$ A; $f - 600$ Hz), (a) Typical TWIH, (b) C-TWIH.

reaches the maximum above the magnetic yokes, while the magnetic flux intensity is relatively weak above the windings. Near the center of axis the intensity decreases to the minimum. The curve of the C-TWIH system's magnetic flux density is relatively more homogeneous than that of typical TWIH heater, which shows low density only in several limited regions. Thus the eddy current field and the temperature field distributions on the work strip should be more uniform in the proposed C-TWIH system than that in typical TWIH systems as confirmed in Part B below.

B. Eddy Current Model Analysis

For the induced eddy current field, the basic equations are established using $\vec{A} - \phi$ formulation. The magnetic vector potential $\vec{A}$ is defined as $\vec{B} = \nabla \times \vec{A}$ and the current density is

$$\vec{J} = -\sigma \left(\frac{\partial \vec{A}}{\partial t} + \nabla \varphi \right) + \vec{J}_s \tag{3}$$

where σ is the electric conductivity; $\vec{J}_s$ is the impressed exciting current density; $\vec{E}$ is the electric field intensity; and

$$\nabla \varphi = -\vec{E} \tag{4}$$

The induced current density in the strip is generated by variations in the magnetic flux. The vortex effects in the strip are attributed to the magnetic fields produced by different structures of typical TWIHs or other types of heaters like TFIH.

By using FEM, the magnetic flux distributions and induced eddy current density in the strip of typical TWIH and C-TWIH systems are shown, respectively, in Fig. 5(a) and (b) for electrical phase angles of 90° and 270°.

It is shown in Fig. 5 that the novel C-TWIH system has a relatively more uniform power density distribution. This is accomplished mainly because of the application of crossed three-phase AC excitations to create uniform magnetic fields that govern the eddy current density distribution. On the other hand, the combination of six induction heaters serves to widen the directions of the induced magnetic field which is distributed along the magnetic yokes. These inductors interact with each other and compensate for the weak magnetic areas existing between the gap districts.

Fig. 6 shows the eddy current density distributions in typical TWIH and C-TWIH systems. As C-TWIH uses crossed three-phase induction heaters, the upper and lower induction heaters are installed properly to compensate for the low-fields so as to realize uniform heating results. It can be seen that the eddy current distributions are more uniform in C-TWIH when compared to those in typical TWIH.

Another characteristic of TWIH systems that needs to be considered is the presence of many high eddy current peaks along the movement directions on the edges of the sheet, which can give rise to, in some cases, dangerous strip deformations. In the proposed C-TWIH system this problem is reduced since sharp peaks of eddy currents are much fewer than those in typical TWIH systems.

The best cases among both typical TWIH and C-TWIH systems, and the transverse flux induction heating (TFIH) system [6], which has the similar geometry, are compared in Fig. 7, where the irregularities due to the use of a relatively small number of mesh elements have been smoothed. It can be seen that from 3 mm to 130 mm, the C-TWIH system induces higher power than any other systems being studied.

C. Thermal Model Analysis

The thermal properties of the materials are functions of temperature. Around the surface of the heating regions, there are dramatic changes in the high temperature zones. In order to improve the accuracy of the simulation, two-dimensional (2-D) nonlinear transient heat conduction equations are introduced to describe the thermal fields.

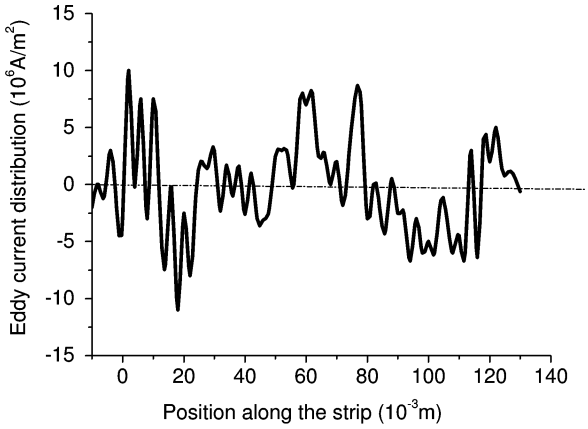

(a)

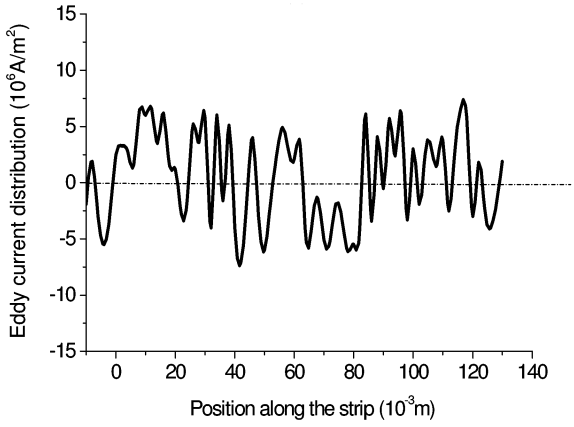

(b)

Fig. 6. Eddy current density distribution in the strip of typical TWIH and C-TWIH systems, (a) Typical TWIH, (b) C-TWIH.

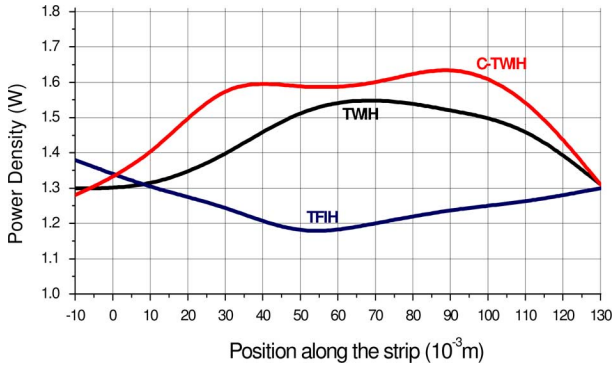

Fig. 7. Relative power density distribution of C-TWIH, TWIH, and TFIH.

Applying eddy current density to be the heat sources during the heating process, the thermal source is

$$P_V = \frac{|\vec{J}|^2}{\sigma} \tag{5}$$

where $\vec{J}$ is the eddy current density and σ is the electric conductivity.

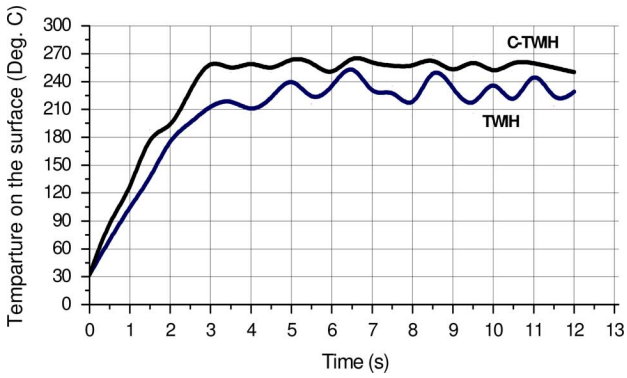

Fig. 8. Temperature distribution along the surface of the strip.

The temperature field is computed based on Fourier's thermal conduction equation

$$\frac{\partial(c\rho\vartheta)}{\partial t} = \nabla\cdot(\lambda\nabla\vartheta) + P_V + \vec{v}\cdot(c\rho\vartheta) \tag{6}$$

where c is the specific heat; ρ is the mass density; λ is the thermal conductivity coefficient; P_V is the thermal source; and $\vec{v}$ is the strip velocity.

Fig. 8 shows that the C-TWIH reaches a higher temperature faster and with fewer variations when compared to typical TWIH. After three seconds, the temperature of typical TWIH is observed to fluctuate between 212°C and 256°C, while C-TWIH has a temperature range from 251°C to 270°C and its unexpected temperature difference is reduced by about 43% compared to that in typical TWIH device.

IV. Conclusion

In this paper, a new crossed traveling wave induction heating (C-TWIH) system is proposed for work strip heating. The simulation results demonstrate that good controllability and efficient thermal transfer can be realized if the choice of the systems and their parameters (inductor geometry, poly-phase winding arrangement and supply, airgap size and control of the relative positions of the inductors) are optimized.

In addition, the proposed C-TWIH system can overcome problems of metal deformation and reduces the noise from the system, where the uniformity of power and eddy currents in the work strips plays an important role.

References

[1] A. L. Bowden and E. J. Davies, "Travelling wave induction heaters design considerations," in *Proc. BNCE-UIE Electroheat Metals Conf.*, England, Sep. 1982, pp. 21–23.

[2] F. Dughiero *et al.*, "Calculation of forces in travelling wave induction heating systems," *IEEE Trans. Magn.*, vol. 31, no. 6, pp. 3560–3562, 1995.

[3] S. Lupi *et al.*, "Comparison of edge-effects of transverse flux and travelling wave induction heating inductors," *IEEE Trans. Magn.*, vol. 35, no. 5, pp. 3556–3558, 1999.

[4] A. Ali *et al.*, "Simulation of multiphase induction heating systems," in *Proc. IEE Conf. Pub.*, 1994, vol. 38, no. 4, pp. 211–214.

[5] Z. M. Wang *et al.*, "Eddy current and temperature field computation in transverse flux induction heating equipment," *IEEE Trans. Magn.*, vol. 37, no. 5, pp. 3437–3439, 2001.

[6] X. G. Yang and Y. H. Wang, "The effect of coil geometry on the distributions of eddy current and temperature in transverse flux induction heating equipment," *Heat Treatment Met.*, vol. 28, no. 7, pp. 49–54, 2003.